5. Simultaneous measurement of ^{222}Rn and its progeny in the presence of ^{220}Rn using Makrofol detectors

As shown in Section 2.3, to well assess the annual radiation dose from exposure to ^{222}Rn progeny in private homes and in workplaces, the information about the equilibrium-equivalent concentration (C_{eq}) integrated over long periods of time (from months to a year) is of great interest. Owing to its simplicity and cheapness, long-term measurement of indoor ^{222}Rn concentration by means of a passive integrating detector, consisting of a NTD enclosed by an inlet filter within a diffusion chamber, is a well-established method used by many laboratories (Miles et al., 1996; Howarth and Miles, 2000a; Howarth and Miles, 2000b). The inlet filter, which protects the enclosed detector from exterior airborne aerosol, dust and moisture as also the ^{222}Rn and/or ^{220}Rn decay products formed outside the diffusion chamber, delays the entry of ^{222}Rn gas into the subsequent sensitive volume ensuring, therefore, the ^{220}Rn discrimination because of its short half-life.

There is a great amount of data of indoor ^{222}Rn levels as a consequence of many surveys carried out around the world with passive integrating detectors (UNSCEAR, 2000). The knowledge of this database gives only a rough estimation of the long-term equilibrium-equivalent concentration (C_{eq}) by assuming a mean equilibrium factor of 0.4 as stated in the ICRP 65 (ICRP, 1994). However, due to local and temporal fluctuations of the processes (ventilation, aerosol concentration, surface deposition, etc.) influencing ^{222}Rn and its progeny concentrations, the assumption of an unique equilibrium factor for any real situation of indoor exposures can result in considerable misinterpretations of the inhalation dose actually accumulated.

Existing data of indoor ^{222}Rn progeny concentrations and, subsequently, of C_{eq} correspond mainly to punctual or short-term measurements with active systems in few sites (Reineking and Porstendörfer, 1990; Peter, 1994; Kies et al., 1996; Ortega and Vargas, 1996; Papp and Daróczy, 1997; Yu et al., 1999; Harley et al., 2000; Yu et al., 2000a; Yu et al., 2000b; Furuta et al., 2000; UNSCEAR, 2000; Yu et al., 2001a). These methods are very useful when the goal is to obtain values of these decay products at a specific time or to analyse their temporal evolution. Otherwise, because of their cost, size, and operating mode, they are not adequate for long-term measurement in a significant fraction of dwelling stock. Accordingly, it would be of great interest to use NTDs to determine the ^{222}Rn daughter concentrations along the same period of time during which the ^{222}Rn concentration is obtained by the diffusion chamber.

5.1. Review of existing passive methods

The first method for ^{222}Rn progeny measurement using NTDs was proposed by Frank and Benton (1977). This method, called *conventional method*, consists of using two NTDs: one enclosed within a diffusion chamber and a second one (open) facing directly the indoor air to be measured. The open detector lets the measurement of the total air α-particle concentration, C_T, of ^{222}Rn+^{218}Po+^{214}Po. By means of the ratio between its reading and that of the enclosed NTD, it is possible to estimate the equilibrium factor as well as the C_p value. This correlation must be done experimentally under well-defined irradiation conditions in pure ^{222}Rn atmospheres. However, the conventional method, which was used by other authors under different system designs and detector configurations (Dománski et al., 1984; Somogyi et al., 1984; Planinic and Faj, 1989; Sarenio and Guhr, 1991), offers not reliable results. Dománski et al. (1984) specifically state its lack of precision and its limited success. The instability of its response is due mainly to the dependence of its reading on the equilibrium factor (Dörschel and Guhr, 1993), on the eventual presence of ^{220}Rn and on the plate-out effects of ^{222}Rn and/or ^{220}Rn decay products above the open detector surface (Maniyan et al., 1999). In addition, this method assumes that the open NTD has the same response (sensitivity) for each of the α-active ^{222}Rn daughter. We will see in Section 6.2.3 that this assumption is not valid in general.

Fleischer (1984) used for ^{222}Rn daughter measurement 4 identical NTDs, three of which are covered by different polyethylene absorber foils of 20 μm, 40 μm and 53.5 μm thick. The bare detector and the first one with 20 μm absorber can register ^{222}Rn+^{218}Po+^{214}Po, whereas those with 40 μm and 53.5 μm absorbers record α-emissions from ^{218}Po+^{214}Po and ^{214}Po, respectively. With this method the α-active daughters (^{218}Po and ^{214}Po) are measured separately and the concentration of the ^{214}Pb (whose β-emissions cannot be

registered by any NTD) is calculated from an inferred diffusion constant, which is chosen to be unidimensional and invariable. This constant is assumed to be the only parameter that controls the daughter distribution indoors. Nevertheless, this method fails since the behaviour of indoor ^{222}Rn progeny near surfaces is influenced by many factors (see, for instance, Section 3.3). For these reasons, Fleischer et al. (1984) put the four NTDs within a special housing box designed to provide unidimensional and uniform air diffusion throughout the passive detectors. The results of this device were, however, not satisfactory. From 7 exposures carried out at the EML exposure facilities, two result in a total disagreement and the method failed. In the other 5 exposures, the measured C_{p} values by the NTDs were 36% higher than those obtained with the active method. In addition, the large dimensions of the diffusion box ($56 \times 56 \times 28$ cm^3) complicate its application for ^{222}Rn progeny measurements in private homes and in workplaces.

Other methods based on measurements of α-track geometric parameters have been developed to carry out α-spectrometry using an open NTD (Hadler and Paulo, 1994; Hadler et al., 1995; Mozzo et al., 1996). Identification and separation of ^{222}Rn, ^{218}Po and ^{214}Po is feasible using these methods. For a given eccentricity (i.e., ratio of the track axis lengths), which is dependent on the angle of incidence, the track area is inversely proportional to the energy of the emitted α-particle. In this sense, it has been shown that by a simultaneous measurement of surface track sizes and its optical property, such as average greyness or brightness, an energy resolution of $\sim$0.1 MeV could be obtained (Ilic and Sutej, 1997; Izerrouken et al., 1999). Nonetheless, this method is very tedious and need the use of very automated and sophisticated track analysis systems.

The α-spectrometry is also viable through the electrochemical etching technique of polycarbonate detectors by varying the pre-etching duration (Al-Najjar et al., 1989; Sohrabi and Sadeghi, 1991). The basis of this technique was adopted in our laboratory to develop, as a first step of this study in order to determine the long-term equilibrium factor, a former method based on a separate measurement of airborne ^{222}Rn and ^{214}Po concentrations using a detector configuration similar to that of the conventional method (Amgarou, 1997; Baixeras et al., 1999a; Baixeras et al., 1999b; Baixeras et al, 1999c). The concept of this method was proposed by Ling (1993) and by Dörschel and Piesch (1993) in which, by fixing the plate-out constants as well as the unattached daughter fractions and by setting correspondences between ventilation and individual concentration ratios, the equilibrium factor is expressed as a function of the ratios of each ^{222}Rn progeny concentrations to that of ^{222}Rn. This method was expected to be much more accurate than the conventional method (Amgarou, 1997; Baixeras et al., 1999a; Dörschel and Piesch, 1994). We have found that, by assuming a relative uncertainty of 10% for the ^{214}Po measurement, a relative uncertainty of about 5-10% in the estimation of the equilibrium factor is obtained; while on the other

hand; if we consider the same uncertainty in the conventional method, the equilibrium factor uncertainty will be about 25-50% (Amgarou, 1997; Baixeras et al., 1999a). The results obtained from indoor application of this method in different private homes and workplaces located in the Barcelona area (Baixeras et al., 1999a; Baixeras et al., 1999b; Baixeras et al., 1999c), indicate that the averaged equilibrium factor agrees with the assumed world mean value (ICRP, 1994). Notwithstanding, the assumption of being the ventilation rate the most relevant parameter is not always a good approximation. Similarly to ventilation, the deposition and aerosol attachment processes depend strongly on the geological features, meteorological conditions, indoor characteristics and inhabitant behaviour causing fluctuations in their values that might be very important and that might lead to considerable fluctuations in the measurement.

To date, the airborne ^{222}Rn progeny measurement by means of NTDs is found to be problematical. In one of the latest intercomparison of passive radon detectors organised by the Commission of the European Communities (Miles et al., 1996), out of 30 measurements carried out by 5 passive detector systems, only one result agreed with active measuring systems. In the following, we present the theoretical basis and the set-up of a new passive integrating system for the simultaneous measurement of ^{222}Rn and its α-emitter progeny (^{218}Po and ^{214}Po) even in the presence of ^{220}Rn. It is based on the fact the half-lives of ^{222}Rn and ^{220}Rn are different, that both isotopes have the same diffusion coefficient in a given medium, and that the NTD response depends on the electrochemical etching conditions used. The general idea of this work is to obtain firstly the long-term equilibrium factor between ^{222}Rn and its airborne progeny from the direct determination of the ^{218}Po and ^{214}Po in air and, then, to calculate the averaged potential α-energy concentration, C_{p}, from the measured value of ^{222}Rn concentration. Moreover, this method lets the estimation of the eventual ^{220}Rn levels. Preliminary results of this study were presented recently at the 20$^{\mathrm{th}}$ International Conference on Nuclear Tracks in Solids (Portoroz, Slovenia) (Amgarou et al., 2001b).

5.2. ^{222}Rn and ^{220}Rn measurement with NTDs

5.2.1. The problem of ^{220}Rn presence

Based on only few and non-representative measurements conducted in the past, most of them carried out with active methods for short periods (ICRP, 1987; UNSCEAR, 2000), it is generally assumed that the ^{220}Rn contribution to indoor radiation dose can be negligible and main concern is primarily focused to ^{222}Rn only. As a result of its relatively short half-life (55.6 s), compared to that of ^{222}Rn (3.83 d), the distance that ^{220}Rn gas

can migrate within a medium before it decays is much shorter than for ^{222}Rn gas and, therefore, it is comparatively easily stopped by wallpaper, paint and other surface sealants. Consequently, the risk for high ^{220}Rn levels indoors may be expected to be low, at least much lower than that for high levels of ^{222}Rn. Nevertheless, in the presence of ineffective barrier between its production site (soil and/or building materials) and indoor air, the entry of ^{220}Rn could be significant. Occasionally high indoor levels of ^{220}Rn gas may occur and the associated effective dose may be sometimes comparable to that of ^{222}Rn (Doi et al., 1994; Yamasaki et al., 1995; Lida et al., 1996; Steinhäusler, 1996; Yu et al., 1999; Pillai and Paul, 1999; Yu et al., 2000a; Yu et al., 2000b; Yu et al., 2001a).

Under such circumstances, as most of ^{222}Rn devices may be also sensitive to ^{220}Rn, the presence of this last may interfere the measurement and may contribute to its overall uncertainty, since all α-counts originated from both isotopes will be attributed erroneously as ^{222}Rn-component only. Moreover, ^{220}Rn concentration decreases exponentially as the distance from its production site increases (Doi et al., 1994; Yamasaki et al., 1995; Lida et al., 1996; Zhuo et al., 2001), so that, ^{222}Rn measurements performed at different positions from the wall will give different values leading to an extra confusion in the actual ^{222}Rn level. This implies that separate measurement of indoor ^{222}Rn and ^{220}Rn concentrations needs to be performed in order to identify sites of considerable high ^{220}Rn levels and to provide useful and precise information concerning the general problem of indoor radiation dose assessment.

5.2.2. Principle of ^{222}Rn and ^{220}Rn measurement with NTDs

^{222}Rn only measurement by means of enclosed NTDs, in an eventual indoor ^{222}Rn and ^{220}Rn indoor air mixture, is properly performed if the filter used is capable to prevent entirely the entry of ^{220}Rn atoms to the diffusion chamber housing without any significant reduction of the actual indoor ^{222}Rn concentration. For this purpose, the filter diffusion coefficient must be relatively low to ensure that the time need for ^{220}Rn atoms to diffuse through such barrier is long enough so that almost all of these atoms decay in the pathway before reaching the sensitive volume of the detector used.

Similarly, precise ^{222}Rn plus ^{220}Rn measurements can be made by the same device as for ^{222}Rn measurement only, with the single substitution of a different permeable filter of a relatively high diffusion coefficient that allows fairly free entry of both isotopes jointly while still keeping out their airborne decay products. The utilisation of two enclosed detectors with two filters of relatively low and high diffusion coefficients side by side allows the separate determination of both ^{222}Rn and ^{220}Rn concentration indoors. Separate measurement of ^{222}Rn and ^{220}Rn can also be carried out by varying only the filter thickness. The only

requirement is that the diffusion coefficient of this filter should be high enough to let the ^{220}Rn entry to the diffusion chamber housing at relatively low thickness.

Decay products formed inside the diffusion chamber cannot leave it and they experiment only the deposition process on its internal wall including the detector surface itself. In this manner, an equilibrium between these products and their associated parent is established within the diffusion chamber. The track formation is, therefore, due to α-emissions produced inside the diffusion chamber. The detector track quantification is related directly to the ^{222}Rn and/or ^{220}Rn gas concentration inside the diffusion chamber, C^{ch}, as follows

$$\rho = \varepsilon \int_0^t C^{\mathrm{ch}}(t)\ \mathrm{d}t \tag{5.1}$$

where ρ (cm^{-2}) is the detector track density and ε (cm^{-2} kBq^{-1} m^3 h^{-1}) its sensitivity.

The ^{222}Rn and/or ^{220}Rn concentration inside the diffusion chamber can be described by the following conservation-of-mass equation (Ward et al., 1977; Fleischer et al., 1980):

$$\frac{\partial C^{\mathrm{ch}}}{\partial t} = -\lambda C^{\mathrm{ch}} + \frac{DS_{\mathrm{f}}}{\delta V^{\mathrm{ch}}}(C - C^{\mathrm{ch}}) \tag{5.2}$$

where C is the actual indoor ^{222}Rn and/or ^{220}Rn concentration to be measured, λ is the ^{222}Rn or ^{220}Rn decay constant, D (cm^2 s^{-1}) is the diffusion coefficient of the filter, S_{f} (cm^2) is the filter surface through which ^{222}Rn and/or ^{220}Rn gas enters the interior volume, V^{ch} (cm^3), of the diffusion chamber and δ (cm) is the filter thickness. The two terms on the right of Equation (5.2) represent (1) the loss due to radioactive decay characterised by mean life $\tau_{\mathrm{R}} = \frac{1}{\lambda}$ and (2) the diffusion through the filter with a mean delay time $\tau_{\mathrm{M}} = \frac{\delta V^{\mathrm{ch}}}{DS_{\mathrm{f}}}$. Taking into account the initial condition of $C^{\mathrm{ch}}(0) = 0$, the build-up of ^{222}Rn and/or ^{220}Rn inside the diffusion chamber becomes (see Figure 5.1)

$$C^{\mathrm{ch}}(t \leq t_0) = \frac{\tau C}{\tau_{\mathrm{M}}}(1 - e^{-\frac{t}{\tau}}) \tag{5.3}$$

where t_0 is the exposure time and the mean time τ is given by

$$\frac{1}{\tau} = \frac{1}{\tau_{\mathrm{R}}} + \frac{1}{\tau_{\mathrm{M}}} \tag{5.4}$$

Consequently, the maximum ^{222}Rn and/or ^{220}Rn concentration inside the diffusion chamber is reduced to a fraction $\frac{\tau}{\tau_{\mathrm{M}}}$ of the outside value for $t >> \tau$. When the exposure is finished, the diffusion chamber is removed from the indoor air to be measured, and is kept temporally in a ^{222}Rn/^{220}Rn-free atmosphere until the enclosed NTD is etched and evaluated. The loss of ^{222}Rn and/or ^{220}Rn into the ^{222}Rn/^{220}Rn-free atmosphere for $t > t_0$ is given by $\frac{\partial C^{\mathrm{ch}}}{\partial t} = -\frac{C^{\mathrm{ch}}}{\tau}$ that may be integrated to give

$$C^{\mathrm{ch}}(t > t_0) = \frac{\tau C}{\tau_{\mathrm{M}}}(1 - e^{-\frac{t_0}{\tau}})e^{-\frac{(t-t_0)}{\tau}} \tag{5.5}$$

By integrating Equations (5.3) and (5.5), the track density ρ is given by

$$\rho(t \leq t_0) = \frac{\tau \varepsilon C t}{\tau_{\mathrm{M}}}\left[1 + \frac{\tau}{t}(e^{-\frac{t}{\tau}} - 1)\right] \tag{5.6}$$

$$\rho(t > t_0) = \frac{\tau^2 \varepsilon C}{\tau_{\mathrm{M}}}(1 - e^{-\frac{t_0}{\tau}})(1 - e^{-\frac{(t-t_0)}{\tau}}) \tag{5.7}$$

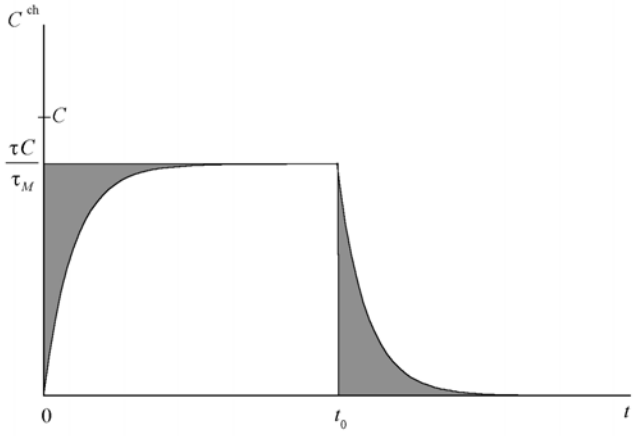

Figure 5.1. Illustration of the build-up and the cooling-off of ^{222}Rn concentration inside the diffusion chamber.

An illustration of the build-up and the loss of ^{222}Rn and/or ^{220}Rn inside the diffusion chamber is given in Figure 5.1. According to this figure, it is seen that the loss of α-counts during the initial phase of diffusion can be compensated if the detector is removed from the diffusion chamber after a certain time lag (the cooling-off period) at the end of the exposure much longer than τ (i.e., $t - t_0 >> \tau$). The integral of the whole curve is the same as for an ideal (rectangular) curve in which the ^{222}Rn and/or ^{220}Rn concentration reaches immediately its maximum possible value at the beginning of the exposure, remains constant during the exposure and drops suddenly to zero at $t = t_0$. However, if the detector is directly removed from the diffusion chamber at the end of the exposure the resulting track density is then $\rho = \frac{\tau \varepsilon C}{\tau_{\mathrm{M}}}(t_0 - \tau)$, i.e., equivalent to an exposure of length $t_0 - \tau$ at a concentration $\frac{\tau \varepsilon C}{\tau_{\mathrm{M}}}$. This correction must be taking into account.

5.3. Equilibrium factor determination using NTDs: a new approach

5.3.1. Theoretical consideration

According to the definition given in Section 2.3, the equilibrium factor between ^{222}Rn and its decay products is given by

$$F_{^{222}\mathrm{Rn}} = 0.105 f_{^{218}\mathrm{Po}} + 0.515 f_{^{214}\mathrm{Pb}} + 0.380 f_{^{214}\mathrm{Bi}} \tag{5.8}$$

where f_i is the disequilibrium degree of the airborne ^{222}Rn daughter i (^{218}Po, ^{214}Pb or ^{214}Bi) and is calculated as the sum $f_i = f_i^{\mathrm{u}} + f_i^{\mathrm{a}}$ (f_i^{u} and f_i^{a} are defined in Section 2.3). In this equation, since the half-life of the ^{214}Po (165 μs) is very small compared to that of the ^{214}Bi (19.9 min) and since the NTDs do not register the β-emissions of this last, both elements are considered as one state. Hereafter, the ^{214}Bi disequilibrium degree ($f_{^{214}\mathrm{Bi}}$) is substituted by that of the ^{214}Po ($f_{^{214}\mathrm{Po}}$). Taking into account Equations (3.20) and (3.21), the aerosol-attached and the airborne-unattached fractions for ^{222}Rn and ^{220}Rn progeny are not independent, and are connected with each other via the recursive formulae

$$f_i^{\mathrm{u}} = \frac{\lambda_i (f_{i-1}^{\mathrm{u}} + p_{i-1} f_{i-1}^{\mathrm{a}})}{\lambda_i + \lambda_{\mathrm{a}} + \lambda_{\mathrm{v}} + \lambda_{\mathrm{d}}^{\mathrm{u}}} \tag{5.9}$$

$$f_i^{\mathrm{a}} = \frac{\lambda_{\mathrm{a}} f_i^{\mathrm{u}} + (1 - p_{i-1})\, \lambda_i f_{i-1}^{\mathrm{a}}}{\lambda_i + \lambda_{\mathrm{v}} + \lambda_{\mathrm{d}}^{\mathrm{a}}} \tag{5.10}$$

As shown in Section 3.5, with the only exception of the decay constants (λ_i) and the recoil factors (p_{i-1}) that have well-known and fixed values, the other parameters (λ_{a}, λ_{v}, $\lambda_{\mathrm{d}}^{\mathrm{u}}$ and $\lambda_{\mathrm{d}}^{\mathrm{a}}$) appearing in Equations (5.9) and (5.10) are highly variable and depend on each indoor environment characteristics. Hence, in this work, these parameters are taken as free parameters whose ranges of variation are given in Table 3.1. Under such circumstances, the disequilibrium degree of each airborne ^{222}Rn decay product can be calculated as a function of these variables as follows

$$f_i = f_i(\lambda_{\mathrm{a}}, \lambda_{\mathrm{v}}, \lambda_{\mathrm{d}}^{\mathrm{u}}, \lambda_{\mathrm{d}}^{\mathrm{a}}) \tag{5.11}$$

Inserting these results into Equation (5.8) we can write also

$$F_{^{222}\mathrm{Rn}} = F(\lambda_{\mathrm{a}}, \lambda_{\mathrm{v}}, \lambda_{\mathrm{d}}^{\mathrm{u}}, \lambda_{\mathrm{d}}^{\mathrm{a}}) \tag{5.12}$$

From these relationships, for each given run of λ_{a}, λ_{v}, $\lambda_{\mathrm{d}}^{\mathrm{u}}$ and $\lambda_{\mathrm{d}}^{\mathrm{a}}$ values, the associated values of the ^{222}Rn progeny disequilibrium degrees as well as the equilibrium

factor are obtained. In consequence, it is possible to establish a one-to-one correspondence between the equilibrium factor and each of the ^{222}Rn daughter disequilibrium degree. To analyse these correspondences, we have plotted in Figure 5.2 the ^{222}Rn progeny equilibrium factor as a function of f_i, $F_{^{222}\mathrm{Rn}} = F(f_i)$, assuming all the possible values for the free parameters λ_a, λ_v, $\lambda_\mathrm{d}^\mathrm{u}$ and $\lambda_\mathrm{d}^\mathrm{a}$. The variation steps chosen for these free parameters were 0.1 h^{-1} for λ_v, 5 h^{-1} for λ_a, 5 h^{-1} for $\lambda_\mathrm{d}^\mathrm{u}$ and 0.05 h^{-1} for $\lambda_\mathrm{d}^\mathrm{a}$.

As the conventional method is based on the ^{222}Rn progeny equilibrium factor estimation from the ratio of the open NTD reading to that of the enclosed NTD, the function $F_{^{222}\mathrm{Rn}} = F(f_\mathrm{T})$, being $f_\mathrm{T} = 1 + f_{^{218}\mathrm{Po}} + f_{^{214}\mathrm{Po}}$, accounting for this method is represented in Figure 5.2 as well. We can observe in this figure that there is not a clear correlation between the ^{222}Rn progeny equilibrium factor and the ^{218}Po disequilibrium degree. The large area obtained for the curve $F_{^{222}\mathrm{Rn}} = F(f_{^{218}\mathrm{Po}})$ makes evidence of its high dependence with respect to the values taken by λ_a, λ_v, $\lambda_\mathrm{d}^\mathrm{u}$ and $\lambda_\mathrm{d}^\mathrm{a}$. Any effort attempting to estimate the ^{222}Rn progeny equilibrium factor from the only measurement of the ^{218}Po disequilibrium degree will never succeed in giving satisfactory results independently on the type of detector used.

In turn, the correlation between the ^{222}Rn progeny equilibrium factor and the ^{214}Pb disequilibrium degree is quite good ($F_{^{222}\mathrm{Rn}} \simeq f_{^{214}\mathrm{Pb}}$) and is not affected by any of the above free parameters. It is very surprising that the function $F_{^{222}\mathrm{Rn}} = F(f_{^{214}\mathrm{Pb}})$ differs so much from the function $F_{^{222}\mathrm{Rn}} = F(f_{^{218}\mathrm{Po}})$. The quite perfect correlation obtained for the function $F_{^{222}\mathrm{Rn}} = F(f_{^{214}\mathrm{Pb}})$ means that the ^{222}Rn progeny equilibrium factor can be obtained with a good precision if separate and accurate measurements of airborne ^{214}Pb concentration is performed together with that of ^{222}Rn. Using this method, the knowledge of the remaining ^{222}Rn decay product concentrations is not necessary and can be obviated. Unfortunately, this method cannot be adopted in this study since the NTDs are insensitive to the β-emissions of this radionuclide.

In contrast to our previous finding (Amgarou, 1997; Baixeras et al., 1999a) and to that obtained by Dörschel and Piesch (1993), the ^{222}Rn progeny equilibrium factor estimation from ^{214}Po disequilibrium degree measurement is not a good approximation. The corresponding function, $F_{^{222}\mathrm{Rn}} = F(f_{^{214}\mathrm{Po}})$, is far from being lineal and presents considerable fluctuations especially at lower values of ^{214}Po disequilibrium degree. These fluctuations may lead to additional uncertainties in the ^{222}Rn progeny equilibrium factor estimation from the ^{214}Po disequilibrium degree. Supposing that there is not any uncertainty associated with the ^{214}Po disequilibrium degree measurement, the uncertainty for the estimation of the ^{222}Rn progeny equilibrium factor is found to vary from 5% at high $F_{^{222}\mathrm{Rn}}$ values ($F_{^{222}\mathrm{Rn}} \geq 0.7$) to 35% at low $F_{^{222}\mathrm{Rn}}$ values ($F_{^{222}\mathrm{Rn}} \leq 0.2$).

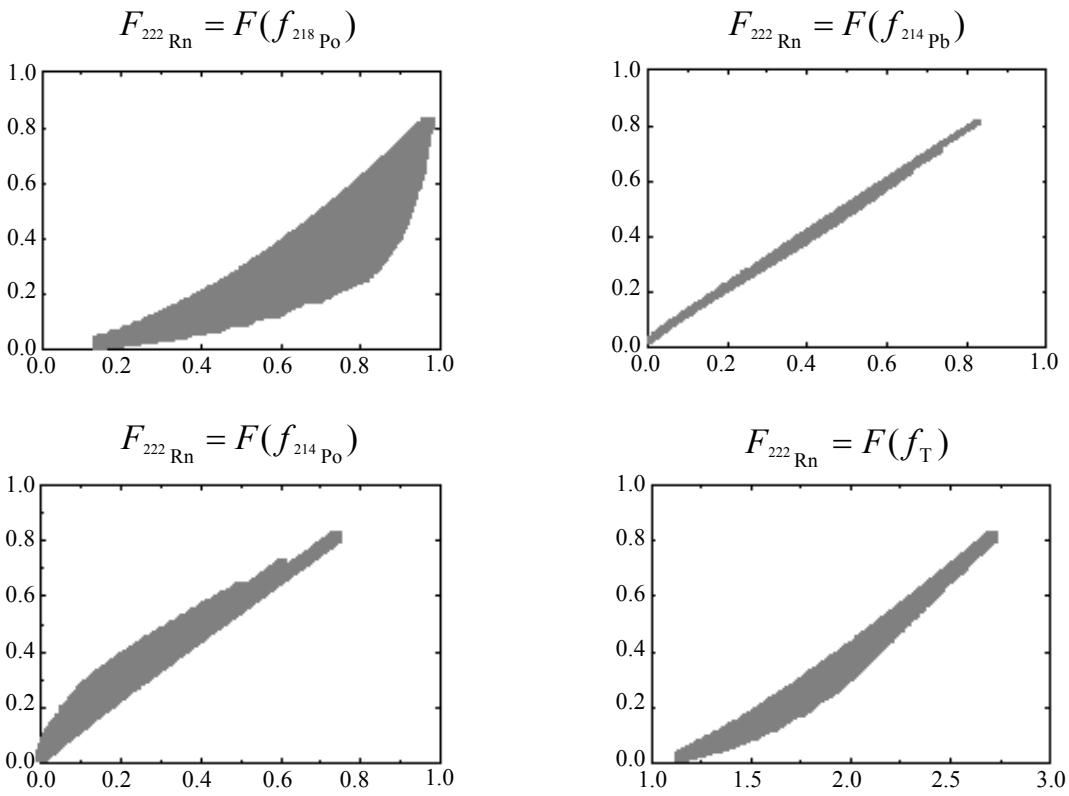

Figure 5.2. ^{222}Rn progeny equilibrium factor vs. the ^{218}Po, ^{214}Pb and ^{214}Po disequilibrium degrees and of the ratio f_{T} assuming all the possible values for the free parameters λ_{a}, λ_{v}, $\lambda_{\mathrm{d}}^{\mathrm{u}}$ and $\lambda_{\mathrm{d}}^{\mathrm{a}}$.

Quasi similar behaviour is found for the conventional method although it presents smaller fluctuations than the function $F_{^{222}\mathrm{Rn}} = F(\, f_{^{214}\mathrm{Po}})$. The corresponding uncertainties found for this method vary from 3% at high $F_{^{222}\mathrm{Rn}}$ values to 25% at low $F_{^{222}\mathrm{Rn}}$ values. The higher precision found previously by our group (Amgarou, 1997; Baixeras et al., 1999a) and by Dörschel and Piesch (1994) for the ^{214}Po method in comparison with the conventional one may be true only where the attachment and the plate-out (attached and unattached) rates are fixed to their baseline values. However, in realistic situations, those rates present high fluctuations, specially the plate-out rate that is a controversial parameter. It has been shown that the correlation between the ^{222}Rn progeny equilibrium factor and the sum $f_{^{218}\mathrm{Po}} + f_{^{214}\mathrm{Po}}$ is analogous to that of the function $F_{^{222}\mathrm{Rn}} = F(f_{\mathrm{T}})$ differing only in the coordinates of each function. All the above results seem to confirm that there is no possibility for an accurate determination of the long-term ^{222}Rn progeny equilibrium factor by means of NTDs.

As the NTDs may register only α-particles emitted from ^{222}Rn, ^{218}Po and ^{214}Po in air, we have considered convenient to define a new quantity, which we have called the *reduced equilibrium factor*, F_{Red}, and which is calculated as

$$F_{\mathrm{Red}} = 0.105\, f_{^{218}\mathrm{Po}} + 0.380\ f_{^{214}\mathrm{Po}} \tag{5.13}$$

By analogy, assuming all the possible values for the variables λ_{a}, λ_{v}, $\lambda_{\mathrm{d}}^{\mathrm{u}}$ and $\lambda_{\mathrm{d}}^{\mathrm{a}}$, the function $F_{^{222}\mathrm{Rn}} = F(F_{\mathrm{Red}})$ is plotted in Figure 5.3 to study the correlation between the two quantities. As clearly shown in this figure, the function $F_{^{222}\mathrm{Rn}} = F(F_{\mathrm{Red}})$ has a similar behaviour as the function $F_{^{222}\mathrm{Rn}} = F(\, f_{^{214}\mathrm{Pb}})$. The dependency between the two quantities $F_{^{222}\mathrm{Rn}}$ and F_{Red} is lineal and the corresponding least-square minimisation fitting gives

$$F_{^{222}\mathrm{Rn}} = 2.2 F_{\mathrm{Red}} - 0.02 \ (\mathrm{R}^2 = 0.996) \tag{5.14}$$

The uncertainties introduced by the fit were found to be less than 0.45%. To test the validity of this equation, we have taken the experimental measurements of indoor ^{222}Rn and its progeny concentrations performed by Reineking and Porstendörfer (1990), under realistic conditions and using active detection systems, in 10 rooms of different German houses. The results of these measurements together with the associated equilibrium factors are shown in Table 5.1. Also given in this table are the corresponding values estimated from the reduced equilibrium factor. The global agreement between the measured equilibrium factor values and those estimated using Equation (5.14) is within 4% and constitutes a reasonable experimental verification of the usefulness of the reduced equilibrium factor concept.

As a direct consequence of this promising finding, long-term ^{222}Rn progeny equilibrium factor can be estimated with the best precision if proper optimisation of experimental conditions for the ^{218}Po and ^{214}Po measurement by means of NTDs, regardless the ^{214}Pb, is performed. In this method, assumptions about ventilation, aerosol attachment and deposition (airborne-unattached and aerosol-attached) rates are not necessary. For this reason, it is desirable for the device to be able to make separate and accurate measurement of ^{222}Rn and its α-active progeny (^{218}Po and ^{214}Po) concentrations using the electrochemical etching technique. A cross check of the consistency of the obtained F-value using this method could be performed by comparing the ^{214}Pb disequilibrium degree value calculated using Equation (5.8) to that estimated from the correlation curve $F_{^{222}\mathrm{Rn}} = F(f_{^{214}\mathrm{Pb}})$.

Table 5.1. The comparison between the equilibrium factors obtained from the Reineking and Porstendörfer (1990) measurements of ^{222}Rn and its progeny concentrations in different German houses and those estimated from Equation (5.14).

Airborne concentration (Bq m^{-3})				Equilibrium factor		
^{222}Rn	^{218}Po	^{214}Pb	^{214}Po	Measured	Eq. (5.14)	% deviation*
52	26	16	13	0.29	0.30	3
206	135	115	99	0.54	0.53	2
215	121	37	25	0.19	0.21	11
253	124	81	73	0.31	0.33	6
260	92	57	52	0.23	0.23	0
300	119	56	45	0.19	0.20	5
329	238	129	108	0.40	0.42	5
331	226	126	113	0.40	0.42	5
333	238	163	125	0.47	0.46	2
366	192	158	134	0.42	0.41	2
430	238	193	189	0.46	0.48	4
454	367	311	282	0.67	0.69	3
456	203	155	148	0.34	0.35	3
594	299	252	248	0.43	0.45	5
740	534	233	152	0.31	0.32	3
764	469	244	179	0.32	0.32	0
785	289	138	101	0.18	0.17	6
846	780	489	344	0.55	0.53	4
876	444	205	172	0.25	0.26	4
940	505	212	151	0.23	0.24	4
943	493	239	199	0.27	0.28	4
1051	510	251	207	0.26	0.26	0
1559	508	293	272	0.20	0.20	0

* calculated as $\left|\frac{\text{Measured - Eq. (5.14)}}{\text{Measured}}\right| \times 100$

In the case of ^{220}Rn and its progeny, the equilibrium factor is given by

$$F_{^{220}\mathrm{Rn}} = 0.914 f_{^{212}\mathrm{Pb}} + 0.086\, f_{^{212}\mathrm{Bi}} \tag{5.15}$$

where $f_{^{212}\mathrm{Pb}}$ and $f_{^{212}\mathrm{Bi}}$ are the ^{212}Pb and ^{212}Bi disequilibrium degrees, respectively. In this equation, the ^{212}Pb is considered as the first daughter of ^{220}Rn since the intermediate α-emitter ^{216}Po has a very relative short half-life (145 ms). This last, although being a solid metal, is in secular equilibrium with its parent (^{220}Rn) and is expected to behave like a gas in airborne-unattached form. Also due to the relative short half-life of the ^{212}Po (300 ns), its concentration is assumed to be 0.64 times that of ^{212}Bi.

Similarly to ^{222}Rn decay products, we have studied the one-to-one correspondence between the equilibrium factor and the disequilibrium degrees of the ^{220}Rn progeny. The results obtained are given in Figure 5.4. As shown in this figure, like the functions $F_{^{222}\mathrm{Rn}} = F(f_{^{214}\mathrm{Pb}})$ and $F_{^{222}\mathrm{Rn}} = F(F_{\mathrm{Red}})$, there is a quasi perfect correlation between ^{220}Rn progeny equilibrium factor and the ^{212}Pb disequilibrium degree. However, again because of being the ^{212}Pb a β-emitter, the function $F_{^{220}\mathrm{Rn}} = (f_{^{221}\mathrm{Pb}})$ cannot be applied to the NTDs. In turn, the function $F_{^{220}\mathrm{Rn}} = (f_{^{221}\mathrm{Bi}})$ shows broad fluctuations and the uncertainties in the estimation of the ^{220}Rn progeny equilibrium factor from the ^{212}Bi disequilibrium degree measurement is about 10-25%. Thus, in contrast to ^{222}Rn decay products, the ^{220}Rn progeny equilibrium factor cannot be estimated with a good accuracy by means of NTDs.

We want to point out that, by the exception of the deposited fractions, the values obtained for the disequilibrium degrees and the equilibrium factor as well as the airborne-unattached and the aerosol-attached fractions of ^{220}Rn daughters are much smaller compared to those obtained for ^{222}Rn decay products. Figures 5.5 and 5.6 show in % the frequency histograms of airborne-unattached, aerosol-attached and deposited fractions of ^{222}Rn and ^{220}Rn progeny, respectively, assuming all the possible values for the free parameters λ_{a}, λ_{v}, $\lambda_{\mathrm{d}}^{\mathrm{u}}$ and $\lambda_{\mathrm{d}}^{\mathrm{a}}$. Also shown in these figures are the associated disequilibrium degrees and the equilibrium factor. In the same manner as for airborne-unattached and aerosol-attached fractions of ^{222}Rn and ^{220}Rn daughters, their deposited fractions were calculated taking into account Equation (3.22). The curves for $f_{^{214}\mathrm{Po}}^{\mathrm{u}}$, $f_{^{212}\mathrm{Pb}}^{\mathrm{u}}$ and $f_{^{212}\mathrm{Bi}}^{\mathrm{u}}$ are not included because they have an unique value equal to zero. According to Figures 5.5 and 5.6, the best fit of the frequency histograms is given by the log-normal distribution functions.

Table 5.2 summarises the geometric means and the ranges of variation of f_i^{u}, f_i^{a}, f_i^{d}, f_i, and F values calculated for ^{222}Rn and ^{220}Rn progeny assuming all the possible values for the free parameters λ_{a}, λ_{v}, $\lambda_{\mathrm{d}}^{\mathrm{u}}$ and $\lambda_{\mathrm{d}}^{\mathrm{a}}$. In this table, the corresponding geometric standard deviations and the correlation factors of the fitted curves are given as well.

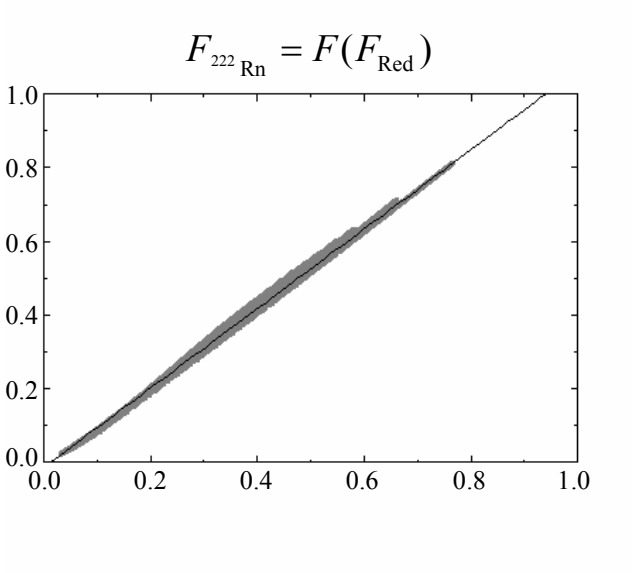

Figure 5.3. ^{222}Rn progeny equilibrium factor, $F_{222_{\mathrm{Rn}}}$, as a function of the corresponding reduced equilibrium factor, $F_{\mathrm{Red}} = 0.105\, f_{218_{\mathrm{Po}}} + 0.380\, f_{214_{\mathrm{Po}}}$, assuming all the possible values for the free parameters λ_{a}, λ_{v}, $\lambda_{\mathrm{d}}^{\mathrm{u}}$ and $\lambda_{\mathrm{d}}^{\mathrm{a}}$. The values of the linear fitting parameters are given in the text.

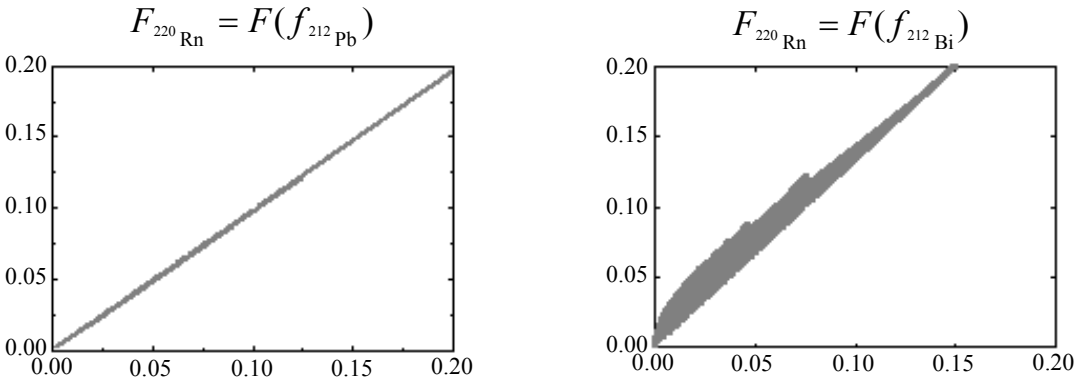

Figure 5.4. ^{220}Rn progeny equilibrium factor vs. the ^{212}Pb and ^{212}Bi disequilibrium degrees assuming all the possible values for the free parameters λ_{a}, λ_{v}, $\lambda_{\mathrm{d}}^{\mathrm{u}}$ and $\lambda_{\mathrm{d}}^{\mathrm{a}}$.

Only the ^{218}Po and ^{214}Pb could be found in airborne-unattached state in private homes and workplaces. However, their airborne-unattached fractions are generally very small — especially that of ^{214}Pb, which is practically inexistent — and do not present any appreciable variation around their geometric mean values. Consequently, the airborne ^{222}Rn and ^{220}Rn decay products are controlled principally by the presence of indoor aerosol particles and the frequency distribution of their disequilibrium degrees are similar to that of the aerosol-attached fractions.

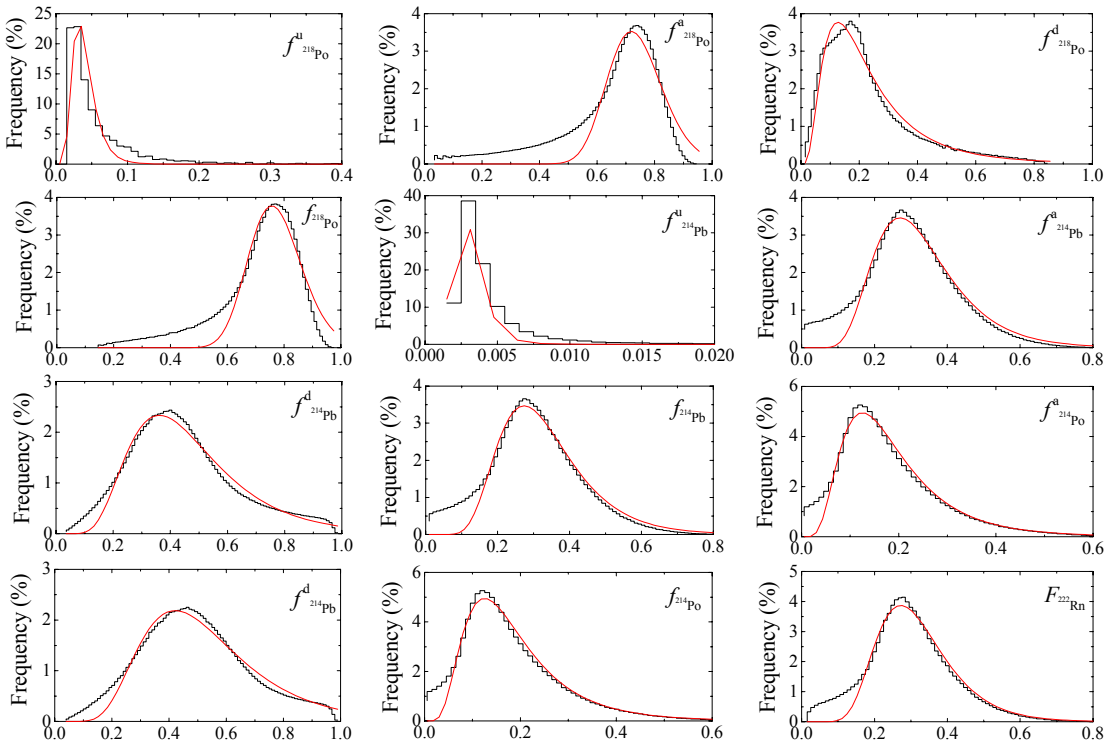

Figure 5.5. Frequency distribution in % of f_i^{u}, f_i^{a}, f_i^{d}, f_i, and F values obtained for ^{222}Rn progeny assuming all the possible values for the free parameters λ_{a}, λ_{v}, $\lambda_{\mathrm{d}}^{\mathrm{u}}$ and $\lambda_{\mathrm{d}}^{\mathrm{a}}$. Data of these curves have been fitted to a log-normal distribution.

Considering the geometric means only, it can be clearly seen that the disequilibrium degrees are very close to the aerosol-attached fractions. These last decrease from one daughter to another along the decay chain direction of ^{222}Rn, while the deposited fractions increase. In the case of ^{220}Rn decay products, the aerosol-attached fractions still decrease

along the decay chain direction but the deposited fractions remain unchanged. This fact could be attributed to the relative long half-life of ^{212}Po (10.64 h). The wide spread ranges of variation found, especially for the disequilibrium degrees as well as for the equilibrium factors of ^{222}Rn and ^{220}Rn progeny, indicate that the assignment of typical values for the free parameters in any realistic case of indoor environment has a large degree of uncertainty.

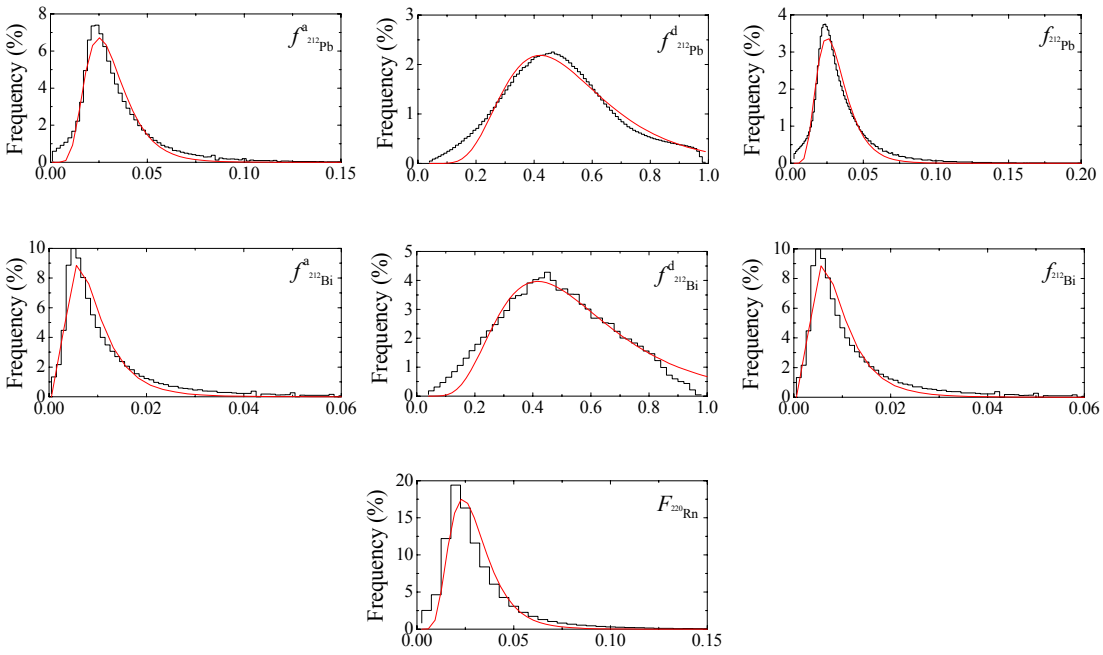

Figure 5.6. Frequency distribution in % of f_i^{u}, f_i^{a}, f_i^{d}, f_i, and F values obtained for ^{220}Rn progeny assuming all the possible values for the free parameters λ_{a}, λ_{v}, $\lambda_{\mathrm{d}}^{\mathrm{u}}$ and $\lambda_{\mathrm{d}}^{\mathrm{a}}$. Data of these curves have been fitted to a log-normal distribution.

5.3.2. Principle of ^{218}Po and ^{214}Po measurement with NTDs

^{222}Rn and its short lived daughters ^{218}Po and ^{214}Po emit, during their radioactive decay, α-particles with initial energies of 5.49 MeV, 6.00 MeV and 7.69 MeV, respectively. Separate measurement of the airborne ^{218}Po and ^{214}Po concentrations requires different α-energy responses for the detector used. However, when exposing a NTD in direct contact with air, the α-emissions of airborne ^{222}Rn and its progeny are slowed down to lower energies during their path to the detector. Thus, for each α-emitter nuclide, α-particles with different energies from 0 up to its initial energy of emission (E_0) may reach the detector surface. To

well optimise the experimental conditions for a separate measurement of the ^{218}Po and/or ^{214}Po concentration in air, the knowledge of the slowing down spectrum of these nuclides in air is of great interest. Taking into account that the straggling effect in the Bragg curve of α-particles (with energy of several MeV) in the air medium is of about 1%, their slowing down spectrum can be obtained from

$$\frac{\mathrm{d}N}{\mathrm{d}E} \propto \frac{1}{(-\frac{\mathrm{d}E}{\mathrm{d}x})} \quad \text{for } E \leq E_0 \tag{5.16}$$

where -$\frac{\mathrm{d}E}{\mathrm{d}x}$ is the stopping power of α-particle in air (see Appendix B). Figure 5.7-A shows, in arbitrary units, the slowing down spectrum curve of the α-particles emitted from ^{222}Rn and its decay products in air[1]. Besides the α-particles emitted from airborne ^{222}Rn and its progeny, the detector may register also the α-emissions of the ^{222}Rn daughters that are plated out directly on its surface. Thus, the slowing down spectrum of Equation (5.16) may be superimposed by two well-resolved peaks corresponding to the initial α-energies of the ^{218}Po (6.00 MeV) and the ^{214}Po (7.67 MeV).

The presence of α-emitter nuclides on the detector surface even in small amounts may considerably alter its response. As previously shown in the Chapter 3, the ^{222}Rn progeny deposition on walls surfaces is a complicate process which depends on several parameters. In addition, it is not possible to identify or reject, at the counting phase, those tracks generated by plate-out effect. As a consequence, the corresponding contribution to the detector reading must be avoided. As clearly illustrated in Figure 5.7-A by a coloured area, separate measurement of the airborne ^{214}Po concentration could be performed if definite upper and lower energy thresholds, namely an α-energy window [$E_{\min}$ - $E_{\max}$], for track registration are conveniently chosen. In this case, the NTD must have a lower energy threshold, $E_{\min}$, above the initial α-energy of the ^{218}Po (6.00 MeV), to avoid both ^{222}Rn and ^{218}Po measurement as well as the plate-out peak of this last. On the other hand, the upper energy threshold, $E_{\max}$, should be below the initial α-energy of ^{214}Po (7.69 MeV) to ensure a total elimination of the corresponding plate-out effect.

In the case of ^{218}Po measurement, any probable α-energy window allowing its detection will register at least a fraction of the ^{214}Po α-particles as well. Likewise, since the upper energy threshold necessary to eliminate the contribution of its plate-out effect will be very close to the initial energy of ^{222}Rn α-emissions, it is not feasible experimentally for the NTDs to obtain an α-energy window that ensures a complete elimination of the ^{222}Rn contribution. Under such circumstance, long-term measurement of the airborne ^{218}Po concentration by means of NTD is viable only if the ^{222}Rn and ^{214}Po concentrations are evaluated separately. In this way, three NTDs are needed to apply this method: one enclosed

[1]The stopping power of the α-particles in air has been calculated using the Srim-2000 code.

within a diffusion chamber to determine ^{222}Rn concentration and a pair open NTDs with different but well-defined α-energy windows for a separate measurement of airborne ^{218}Po and ^{214}Po. For practical reasons, the upper and lower energy thresholds for airborne ^{218}Po determination could be chosen to be similar to that used for ^{222}Rn measurement with enclosed NTD (see the next section).

Table 5.2. The geometric means and the ranges of variation of f_i^{u}, f_i^{a}, f_i^{d}, f_i, and F values obtained for ^{222}Rn and ^{220}Rn progeny assuming all the possible values for the free parameters λ_{a}, λ_{v}, $\lambda_{\mathrm{d}}^{\mathrm{u}}$ and $\lambda_{\mathrm{d}}^{\mathrm{a}}$ as well as their geometric standard deviations (σ_{g}) and the corresponding correlation factors (R^2) of the fitted curves.

	^{222}Rn progeny			^{220}Rn progeny	
	^{218}Po	^{214}Pb	^{214}Po	^{212}Pb	^{212}Bi
f_i^{u}	0.04 (0 - 0.2) $\sigma_{\mathrm{g}} = 1.5$ $\mathrm{R}^2 = 0.94$	0.003 (0 - 0.01) $\sigma_{\mathrm{g}} = 1.4$ $\mathrm{R}^2 = 0.98$	0	0	0
f_i^{a}	0.7 (0 - 0.9) $\sigma_{\mathrm{g}} = 1.1$ $\mathrm{R}^2 = 0.87$	0.3 (0 - 0.7) $\sigma_{\mathrm{g}} = 1.5$ $\mathrm{R}^2 = 0.92$	0.2 (0 - 0.5) $\sigma_{\mathrm{g}} = 1.7$ $\mathrm{R}^2 = 0.96$	0.03 (0 - 0.1) $\sigma_{\mathrm{g}} = 1.5$ $\mathrm{R}^2 = 0.98$	0.01 (0 - 0.04) $\sigma_{\mathrm{g}} = 1.8$ $\mathrm{R}^2 = 0.98$
f_i^{d}	0.2 (0 - 0.8) $\sigma_{\mathrm{g}} = 2.0$ $\mathrm{R}^2 = 0.98$	0.5 (0 - 1) $\sigma_{\mathrm{g}} = 1.6$ $\mathrm{R}^2 = 0.96$	0.5 (0 - 1) $\sigma_{\mathrm{g}} = 1.5$ $\mathrm{R}^2 = 0.98$	0.5 (0 - 1) $\sigma_{\mathrm{g}} = 1.5$ $\mathrm{R}^2 = 0.96$	0.5 (0 - 1) $\sigma_{\mathrm{g}} = 1.6$ $\mathrm{R}^2 = 0.94$
f_i	0.8 (0.2 - 0.9) $\sigma_{\mathrm{g}} = 1.1$ $\mathrm{R}^2 = 0.90$	0.3 (0 - 0.7) $\sigma_{\mathrm{g}} = 1.5$ $\mathrm{R}^2 = 0.94$	0.2 (0 - 0.5) $\sigma_{\mathrm{g}} = 1.7$ $\mathrm{R}^2 = 0.94$	0.03 (0 - 0.1) $\sigma_{\mathrm{g}} = 1.5$ $\mathrm{R}^2 = 0.98$	0.01 (0 - 0.04) $\sigma_{\mathrm{g}} = 1.8$ $\mathrm{R}^2 = 0.98$
F		0.3 (0 - 0.7) $\sigma_{\mathrm{g}} = 1.4$ $\mathrm{R}^2 = 0.96$		0.03 (0 - 0.1) $\sigma_{\mathrm{g}} = 1.5$ $\mathrm{R}^2 = 0.98$	

Last but not least, indoor ^{220}Rn may occur as well as ^{222}Rn and, according to the previous section, there is always a considerable fraction of its decay products able to plate-out on the available surfaces as well as that of the detector itself. However, as shown in Figure 5.7-B, the plate-out peaks of ^{212}Bi and ^{212}Po with initial α-energies of 6.07 MeV and 8.78 MeV, respectively, do not overlap the ^{218}Po and ^{214}Po α-energy windows. Thus, in the case of long-term measurements of airborne ^{218}Po and ^{214}Po concentrations, the open NTDs used is not altered by the plate-out effect on their surface of ^{222}Rn and ^{220}Rn progeny.

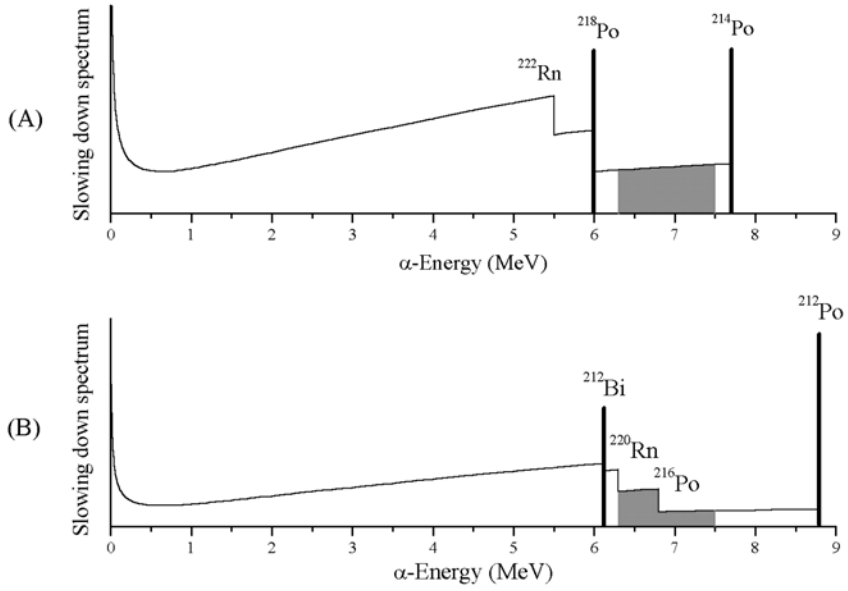

Figure 5.7. Slowing down spectrum in arbitrary units due to ^{222}Rn (A) and ^{220}Rn (B) α-emitter progeny in air and the corresponding peaks of the plate out effect on the detector surface. The coloured area shows the α-energy window response necessary for the NTDs to measure the airborne ^{214}Po concentration.

5.4. Detector system design

The prototype passive integrating system used in this study for ^{222}Rn and its α-emitter progeny measurement in the presence of ^{220}Rn consists of:

1. two Makrofol (type DE with a thickness of 500 μm) detectors, namely detectors A and B, which are enclosed within two diffusion chambers — each one with different filter membrane — to measure indoor ^{222}Rn+^{220}Rn and ^{222}Rn, respectively, and

2. two Makrofol detectors (C and D) that are kept in direct contact with air and that are electrochemically etched at different conditions to obtain the airborne ^{218}Po and ^{214}Po concentrations.

As a diffusion chamber, the so-called FzK[2] dosimeter with a hemispherical housing of 1.5 cm radius (Urban, 1986) is selected. This dosimeter has been widely used by our group to measure the time-averaged concentration of ^{222}Rn in private homes and in some workplaces (Gutiérrez et al., 1992; Baixeras et al., 1996). The filters of the enclosed detectors

[2]FzK is an abbreviation of the Forschungzentrum Karlsruhe centre, Germany, formerly known as Kernforschungzentrum Karlsruhe (KfK) centre.

A and B have relatively high and low diffusion coefficients, respectively. Accordingly, only the noble gas components — ^{222}Rn+^{220}Rn in the first case and ^{222}Rn in the second case — are able to enter the hemispherical housing. The two filters together with their respective enclosed detectors are fixed by a holder ring and are pressed when assembling the FzK diffusion chamber. With the small dimension of the hemispherical housing, an homogeneous distribution inside the diffusion chamber can be assumed. Furtherwise, it has been found that the detector response for small diffusion chambers is independent on the partitioning state (volume-distributed or surface-deposited) of ^{222}Rn and ^{220}Rn daughters within it (Somogyi et al., 1984). The components of the FzK diffusion chamber are made from an electrically conductive plastic to avoid anisotropic deposition of ^{222}Rn and/or ^{220}Rn progeny on the inner housing walls. All the Makrofol detectors used have a circular shape of 2.1 cm diameter and are coated with aluminised Mylar foil of 3 μm thick to avoid the creation of static charge on their surface that may enhance the deposition of ^{222}Rn and ^{220}Rn decay products. Given the characteristics of the FzK diffusion chamber only α-particles with energies above 3.5 MeV reach the enclosed detector (see, for instance, Section 6.2.4).

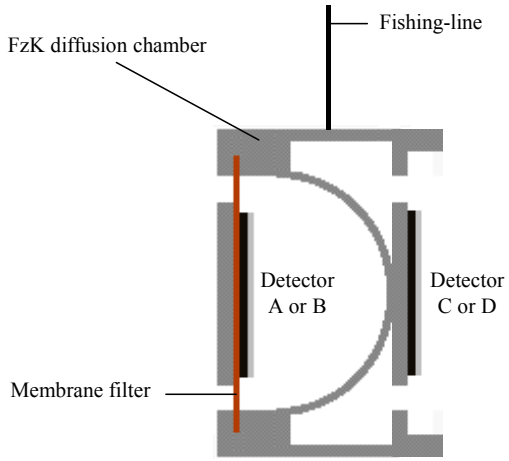

Figure 5.8. The design of the passive integrating system used to measure ^{222}Rn and its α-emitter progeny in the presence of ^{220}Rn.

The development of a suitable detector system design has been carried out by defined tests of various geometries, arrangements and positions of the detectors. As a result of these tests, the optimum detector system design proposed is shown in Figure 5.8. It consists of the adaptation of the FzK diffusion chamber in two identical combinations. In each combination, namely A + C and B + D, each open detector is fixed at the back of a diffusion chamber. The conjunct, with a cylindrical shape of 4 cm diameter and 3 cm

height, is held by a fishing-line in a horizontal position, away from any other surfaces that may disturb the registration process of the open detectors.

Two α-energy windows of interest are chosen, one from 3.0 to 5.0 MeV for the detector A, B and C and another one from 6.3 to 7.5 MeV for the detector D. With these α-energy windows, the detector B lets the measurement of ^{222}Rn concentration. The concentration of ^{220}Rn can be obtained as a response difference of the detectors A and B. The reading of detector D allows the determination of the airborne ^{214}Po concentration. From this quantity and the information given by the detector C the airborne ^{218}Po concentration can be determined.